

This work was written as part of one of the author's official duties as an Employee of the United States Government and is therefore a work of the United States Government. In accordance with 17 U.S.C. 105, no copyright protection is available for such works under U.S. Law.

Public Domain Mark 1.0

<https://creativecommons.org/publicdomain/mark/1.0/>

Access to this work was provided by the University of Maryland, Baltimore County (UMBC) ScholarWorks@UMBC digital repository on the Maryland Shared Open Access (MD-SOAR) platform.

Please provide feedback

Please support the ScholarWorks@UMBC repository by emailing scholarworks-group@umbc.edu and telling us what having access to this work means to you and why it's important to you. Thank you.

Total ozone/UVB monitoring and forecasting: Impact of clouds and the horizontal resolution of satellite retrievals

J. R. Ziemke,^{1,2} J. R. Herman,³ J. L. Stanford,⁴ and P. K. Bhartia³

Abstract. This study compares the horizontal resolution of solar backscatter ultraviolet 2 (SBUV2) total ozone (Ω) fields with those from the new NASA earth probe (EP) and Advanced Earth Observing Satellite (ADEOS) total ozone mapping spectrometer (TOMS) side-scanning photometers. The latter instruments provide high resolution, easily resolving the medium-scale waves (4–7 wavelengths around the Earth at a fixed latitude) that dominate day-to-day midlatitude Ω fluctuations. In contrast, SBUV2 instruments do not, since these devices measure only at nadir (straight downward), yielding ~ 14 measurements daily at a given latitude. This method has consequences not only for global monitoring of Ω and ultraviolet B (UVB, 290–320 nm), but also for short-timescale Ω and UVB predictions in summer because timescales of a few days are coupled to medium horizontal scales (several thousand kilometers) by baroclinic waves that typically force the observed Ω variations. We use a simple Ω prediction model to test the use of Ω fields from TOMS and SBUV instruments and show that the higher zonal resolution from side-scanning TOMS instruments results in sizeable reductions in Ω prediction errors, whereas predictions using SBUV2 Ω are no better than persistence (where tomorrow's Ω is taken to be today's) in the biologically important summer months. Daily variabilities (equivalent to errors in 24-hour persistence forecasting of Ω) in high-resolution TOMS midlatitude ozone during summer are shown to sometimes exceed 50 Dobson units, producing daily changes of 20% or greater in computed ground-level clear-sky UV index. This study demonstrates that even these large daily changes in measured or predicted clear-sky UV are usually smaller than daily UV changes associated with transient clouds. While surface UVB variability is dominated by local cloudiness variations, Ω forecasts can enhance UVB prediction in relatively cloud free regions such as the U.S. desert southwest and in stagnant high-pressure regimes that can persist for 1–2 weeks in summer. Furthermore, as weather forecast models increase in accuracy of forecasted cloudiness, accurate predictions will allow more accurate UVB forecasts for cloud free regions, the locations where they are most needed. Results from the present paper show, however, that high-resolution TOMS-like side-scanning Ω measurements are required for ozone and UVB monitoring and prediction, rather than SBUV-type nadir observations.

1. Introduction

Loss of stratospheric ozone outside the tropics within the last decade has spawned a greater awareness and concern regarding the determination of ground-level ultraviolet B (UVB, wavelengths 290–320 nm) radiation. These wavelengths can produce significant bio-

logical damage, including DNA at the shorter wavelengths [e.g., *Madronich*, 1993]. Because solar UV is absorbed mostly by ozone in the stratosphere, variabilities in UVB depend strongly on variabilities in total column ozone (Ω). The behavior is also highly dependent upon UV wavelength. In midlatitudes during summer a -10% change in Ω yields roughly a +2% change in surface UV at 320-nm wavelength, while at 290 nm the same ozone change yields approximately a +110% change in UV.

A number of recent studies have presented methods for predicting Ω (either regional or global) on timescales of hours to several days based on statistical correlations between Ω and meteorological variables, using forecasts of the latter [*Burrows et al.*, 1994; *Austin et al.*, 1994; *Spankuch and Schulz*, 1995; *Long et al.*, 1996; *Stanford and Ziemke*, 1996; *Ziemke and Stanford*, 1998;

¹Software Corporation of America, Lanham, Maryland.

²Also at NASA Goddard Space Flight Center, Greenbelt, Maryland.

³NASA Goddard Space Flight Center, Greenbelt, Maryland.

⁴Department of Physics and Astronomy, Iowa State University, Ames.

Copyright 1998 by the American Geophysical Union.

Paper number 97JD03324.

0148-0227/98/97JD-03324\$09.00

Atkinson *et al.*, 1998]. For example, daily forecasts of northern hemisphere (NH) UVB derived from predicted Ω fields are currently provided by the U.S. National Weather Service (NWS) in collaboration with the U.S. Environmental Protection Agency (EPA) [Long *et al.*, 1996]. The primary purpose is to provide predictions of UVB 24 hours in advance, by combining daily total ozone measurements from the solar backscatter ultraviolet (SBUV) satellite instrument with National Centers for Environmental Prediction (NCEP) meteorological analyses. SBUV-class instruments have played an important role in long-term ozone trend studies and fly on operational meteorological satellites. These instruments make only nadir (straight downward) ozone observations, consequently limiting zonal resolution to about 14 observations around a latitude circle each day. Besides SBUV, the TIROS operational vertical sounder (TOVS) provides another global field of Ω used by the U.S. NWS in forecasting UVB. TOVS is a side-scanning instrument that provides greater horizontal resolution than SBUV. However, NCEP temperatures are used to produce the TOVS ozone fields, and a subsequent data bias has been recognized between ozone and temperature used in the model. In consequence, TOVS ozone is usually used only as a backup when SBUV measurements are unavailable [Long *et al.*, 1996].

The technique used by the U.S. NWS is a regression that employs daily increments of SBUV (and TOVS) total ozone, NCEP temperatures, and NCEP geopotential heights. Results shown by Long *et al.* [1996] indicated around 10% reduction of RMS errors (relative to persistence, where tomorrow's ozone is taken to be today's) in the NH during winter, when stratospheric dynamics is dominated by long planetary scales (waves 1-3). During the biologically important summer months the technique does not appear to do better than forecasts based on using simple persistence. As we show in the present paper, this result arises from SBUV zonal sampling coupled with the occurrence of medium-scale (zonal wavenumbers 4-7) and shorter propagating waves.

SBUV total ozone data are compared in this study with analyses from three Ω side-scanning satellite instruments that offer higher horizontal resolution: Nimbus 7, earth probe (EP), and Advanced Earth Observing Satellite (ADEOS) total ozone mapping spectrometer (TOMS). There are distinct differences between SBUV and TOMS total ozone measurements. For nadir-viewing SBUV the instrumental field of view (FOV) covers an area on the Earth's surface of effective diameter around 200 km; in contrast, this is approximately 25 km for EP and 50 km for both Nimbus 7 and ADEOS. For SBUV, each orbit provides around 90-100 nadir measurements. In comparison, Nimbus 7, EP, and ADEOS all provide roughly 14,000 measurements each orbit because these instruments are side scanners. The result is much greater horizontal resolution for these TOMS instruments (nearly complete global coverage for both Nimbus 7 and ADEOS TOMS, excluding polar night latitudes). However, unlike the

TOMS instruments, SBUV sacrifices horizontal resolution for measurements of ozone vertical profiles; these profiles are most accurate at altitudes above the ozone number density peak (~20-25 km altitudes) [Fleig *et al.*, 1990; Bhartia *et al.*, 1996].

This study also compares TOMS and SBUV ozone data for use as initialization fields in a simple next-day ozone prediction model. Our primary goals are to examine (1) the effect of horizontal resolution of satellite Ω retrievals on global monitoring and next-day ozone and UVB predictions and (2) the relative impact of UV-shielding clouds, which are presently difficult to predict.

2. Total Ozone Prediction Method

Several investigations, including those from weather service organizations worldwide, have described unique methods for forecasting Ω [Burrows *et al.*, 1994; Austin *et al.*, 1994; Spankuch and Schulz, 1995; Long *et al.*, 1996; Stanford and Ziemke, 1996; Ziemke and Stanford, 1998; Atkinson *et al.*, 1998]. In this study we focus on using a simple approach as described by Stanford and Ziemke [1996].

Two regression models were examined by Stanford and Ziemke [1996] (hereinafter SZ) to predict clear-sky Ω from dynamical variables. The first used a single-parameter model with 50-100 hPa (~16-20 km altitude) temperature as the dependent variable:

$$\Omega_t = \Omega_{t_0} + \gamma \cdot [T_t - T_{t_0}]. \quad (1)$$

Subscript t in (1) denotes forecast day, t_0 is initialization day, T is temperature, Ω is in Dobson units (1 DU = 10^{-5} m vertical thickness of ozone gas at 273.15 K and 1013.25 hPa pressure), and γ is a local (latitude, longitude) day-indexed regression coefficient evaluated for each month (see SZ for a table of γ and other details). This single-parameter model involved regression using several years of Nimbus 7 version 7 TOMS ozone and NCEP temperatures, resulting in a simple lookup table approach to 24-hour predictions.

The second model used by SZ was similar to the method used by the U.S. NWS and was based on backward spatial regressions (2-day means) using global hemispheric fields (30°-60° latitude bands) of 100- and 500-hPa geopotential heights and 50-hPa temperatures as database. (The regression was an extension of (1) above using these three variables with separate γ coefficients.) Results showed that both methods provided improved 24-hour predictions of Ω over persistence for both summer hemispheres. The present paper compares 24-hour predictions of Ω for both TOMS and SBUV, using the single-parameter method from (1).

3. Data

Total ozone used in this study includes (for 1989-1992) Nimbus 7 version 7 TOMS and NOAA 11 SBUV2 and also (for 1996) NOAA 14 SBUV2, EP, and ADEOS TOMS instruments. (Unfortunately, ADEOS became

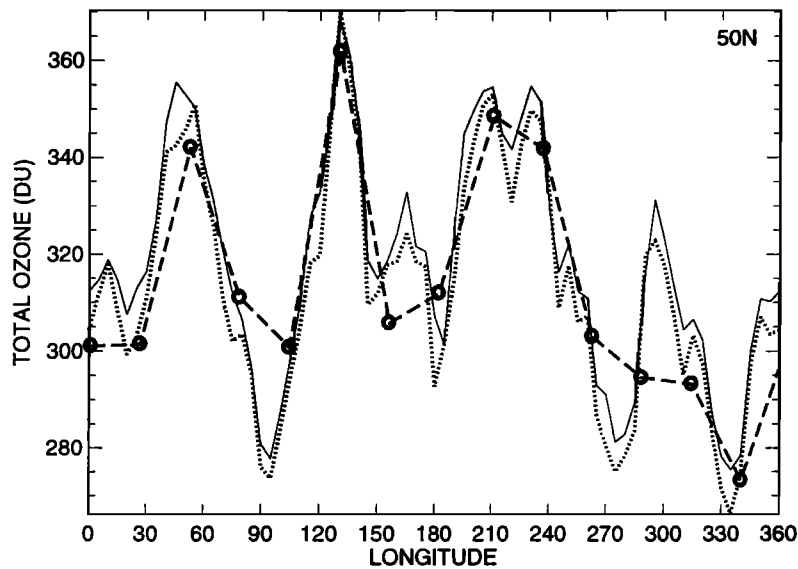


Figure 1. Total ozone (in Dobson units) plotted versus longitude on September 21, 1996, at 50°N as measured by NOAA 14 SBUV2 (circles), EP TOMS (dotted curve), and ADEOS TOMS (solid curve) instruments. SBUV2 longitudes and total ozone values were linearly interpolated from nearest nadir measurements north and south of 50°N.

nonfunctional in late June 1997.) Temperature fields were obtained from daily (1200 UTC) NCEP analyses. Initial fields from all TOMS data were on high-density (HD) 1° latitude \times 1.25° longitude grids. Data were binned further to a medium-density (MD) resolution of 2° latitude \times 5° longitude blocks. A low-density (LD) format was also derived using 5° latitude (85°S to 85°N) \times 15° longitude blocks. These latter fields were tested by using (1) against similar gridded SBUV data. Data from the LD gridding still retain most of the variance in Ω , providing measurements of zonal variabilities up to zonal wave 12.

4. Aliasing in SBUV Measurements

Figure 1 compares longitudinal variations of Ω at 50°N on September 21, 1996, as measured by EP TOMS, ADEOS TOMS, and NOAA 14 SBUV2 instruments. Ω variations of the order of 20–30% occur about the zonal mean (\sim 316 DU) at this midlatitude location. Time series comparisons show that these variations have short timescales of a few days. Figure 1 reveals that EP and ADEOS TOMS agree closely with each other, generally to within about 1% (ADEOS being consistently

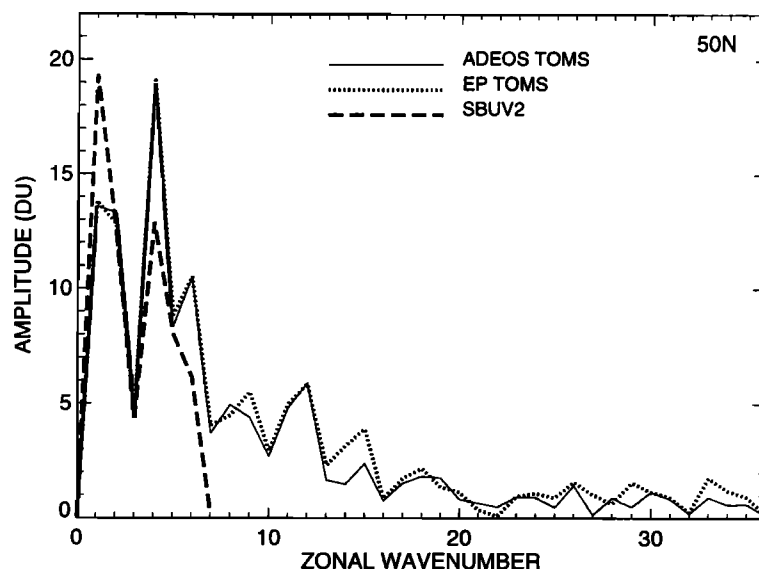


Figure 2. Fourier raw (nonsmoothed) spectral amplitudes (in Dobson units) versus zonal wavenumber for the data shown in Figure 1. Zonal means were subtracted from data prior to analysis. Fourier amplitudes for SBUV2 (bold dashed curve) were derived after linearly interpolating SBUV2 data in Figure 1 to 360 points along longitude. SBUV2 is plotted only up to the Nyquist fold at wavenumber 7.

larger), while SBUV2 misses most zonal variability because of its low-resolution nadir sampling (~ 14 observations around a latitude circle each day).

Figure 2 shows the results of Fourier analyzing the Ω data in Figure 1 into zonal wavenumber components. Medium-scale waves (zonal wavenumbers 4–7, zonal wavelengths of ~ 4000 – 6000 km) dominate the Ω field at midlatitudes and are seen to be insufficiently captured with the lower resolution available from the SBUV2 measurements. Medium-scale Ω fluctuations are ubiquitous in midlatitudes of both hemispheres during summer and are typically forced by upper tropospheric/lower stratospheric anomalies associated with baroclinic disturbances. For example, the southern hemisphere (SH) summer upper tropospheric and lower stratospheric circulation patterns are generally dominated by medium-scale waves [Randel and Stanford, 1985]. Note that SBUV2 cannot resolve ozone variance beyond the Nyquist fold near wave 7. Moreover, because the latter variance must appear somewhere, it is aliased into waves 1–7. While both EP and ADEOS TOMS show a dominant wave 4 and weaker wave 1, SBUV2 measurements indicate just the opposite because of data sampling/aliasing. Possible ozone signals aliasing into wave 1 and wave 4 in SBUV2 are given by zonal wavenumbers $14m \pm 1$ and $14m \pm 4$ ($m=1,2,3,\dots$), respectively.

5. Comparison of Ozone Predictions Using SBUV and TOMS

The results above suggest that the horizontal sampling of Ω measured by nadir-sounding SBUV may be insufficient for short-range ozone and UV prediction models. To test this hypothesis, we compared Ω predictions using Nimbus 7 TOMS and NOAA 11 SBUV2 fields in the model regressions. We used the SZ model (1) that utilizes strong positive correlations between Ω and 50- to 100-hPa mean lower stratospheric temperatures.

Figure 3 shows standard temporal correlations for TOMS and SBUV2, as a function of zonal wavenumber and latitude, with lower stratospheric 50- to 100-hPa NCEP mean temperatures. Correlations were calculated each month at each grid point by using daily time series for 1989–1992 for each individual zonal wavenumber followed by zonal averaging. To condense results, all months were averaged together. The correlation patterns in Figure 3 are the same for summer-only months, except for slightly larger correlations (> 0.8) in the summer hemispheres (figures not shown).

Correlation amplitudes for TOMS (Figure 3a) are largest in medium-scale waves 4–7 and fall off north and south from midlatitudes. In contrast, Figure 3b shows that SBUV2 Ω correlations are considerably weaker and occur at lower wavenumbers (longer zonal scales), a direct result of the lower horizontal resolution and consequent aliasing inherent in SBUV2 measurements. Dynamical parameters such as lower stratospheric tem-

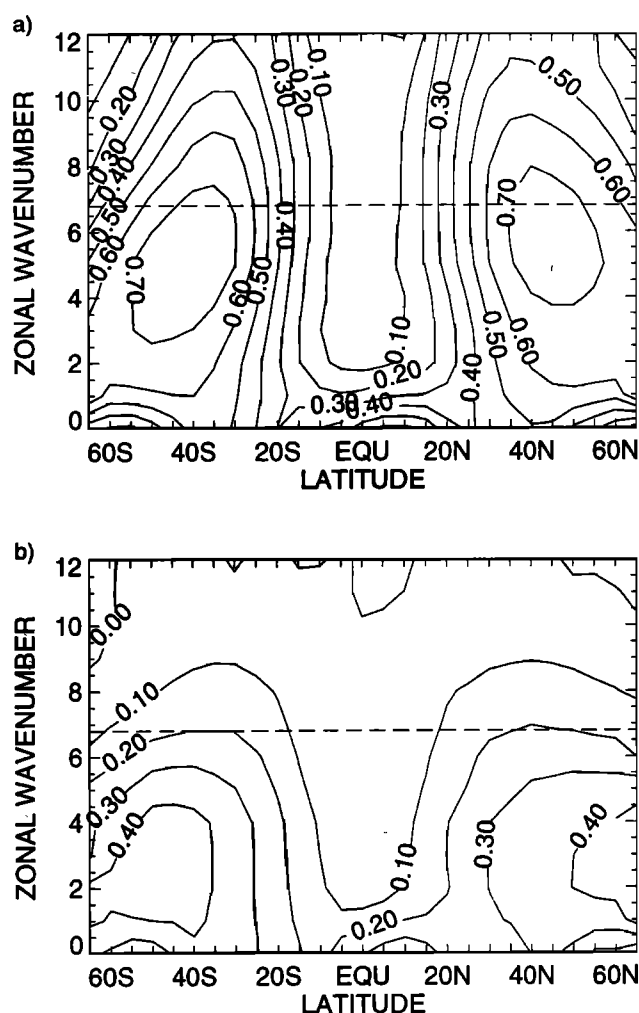


Figure 3. (a) Temporal correlations between Nimbus 7 version 7 TOMS total ozone and 50- to 100-hPa mean NCEP temperatures for 1989–1992 as a function of zonal wavenumber and latitude. Contour increments are 0.1. Correlations were calculated each month from daily data and then averaged over all 48 months. Critical correlation amplitudes [Hogg and Craig, 1978] for a single month of length 30 days are 0.36, 0.56, and 0.64 for significance levels 5%, 0.1%, and 0.01%, respectively. The horizontal dashed line identifies the Nyquist fold near wave 7 for SBUV2. (b) Same as Figure 3a, but with NOAA 11 SBUV2 in place of Nimbus 7 TOMS.

peratures are limited in their usefulness for predicting next-day Ω because Ω is not a conserved atmospheric tracer. Rather, it is a total column measurement that encounters constant transport effects, such as column deformity caused by stratospheric wind shears.

In Ω forecast models, predictions are usually made only a few hours, and usually up to at most 24 to 48 hours, in advance. Predictions of next-day ozone based on the SZ model (1) are compared against persistence using LD-gridded Nimbus 7 TOMS and NOAA 11 SBUV2 in Figure 4. The persistence errors (bold curves) are equivalent to daily variabilities in TOMS ozone as discussed by Allen and Reck [1997]. For comparison, also shown (top curves, discussed in section 6)

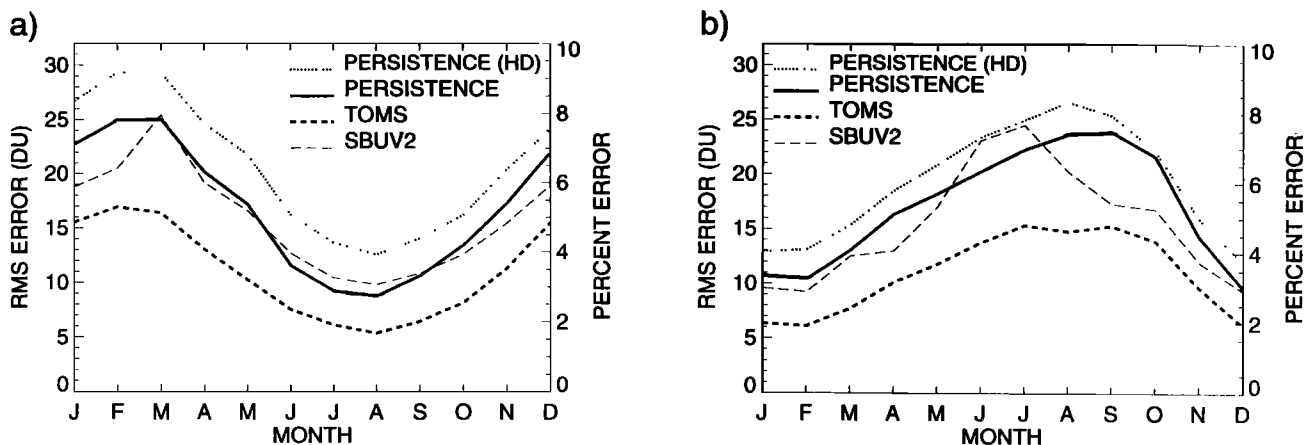


Figure 4. (a) Comparison of 1-day LD total ozone prediction errors for persistence (bold solid curve) and Nimbus 7 TOMS (bold dotted curve) and NOAA 11 SBUV2 (long dashed) using (1) (see section 2). Also shown (top curves) are prediction errors using the persistence method applied only to HD-gridded TOMS data. The γ coefficients in (1) were computed individually for TOMS and SBUV2 and averaged for 1989–1990. RMS errors (in Dobson units) shown on left axes are averaged monthly from 1991 to 1992 for 30°–60° latitudes in (a) northern hemisphere and (b) southern hemisphere. Also shown (right-hand axes) are these errors in percent of month-to-month Nimbus 7 TOMS 1979–1992 zonal mean climatology. Each month consists of 28 separate 1-day forecast simulations; initialization day for each consecutive forecast is incremented by 1 day, up to 28.

are prediction errors using the persistence method applied only to the HD-gridded TOMS data set.

RMS errors in Figure 4 were computed from the difference between the next-day forecast for Ω at a given latitude–longitude location and Ω observed there by TOMS on the forecast date. As indicated, model initialization using TOMS Ω (bold dashed curves) results in obvious reduction in prediction errors each month, whereas use of the lower-resolution SBUV2 data (long dashed curves) does not. All prediction errors are smallest during summer months in both hemispheres, just when UVB forecasts are most beneficial. In winter and spring, RMS errors are largest and coincide with the seasonal occurrence of strong planetary waves in the stratosphere.

6. Clouds and UV Forecasts

Figure 4 showed that 1-day predictions using simple persistence of LD-gridded TOMS (bold curves) yielded errors of around 3–4% (relative to background Ω during summer months). In comparison, the much higher resolution HD-gridded TOMS data (top curves in Figure 4) indicated persistence errors that were only marginally larger, by 1% or less. Hence regardless of whatever method is used to predict clear-sky ozone, on average the largest possible error reductions during summer months are at most 4–5% of background Ω .

However, during summer it is not uncommon to observe large local day-to-day variabilities in Ω [Allen and Reck, 1997]. Figure 5 shows histograms of accumulated

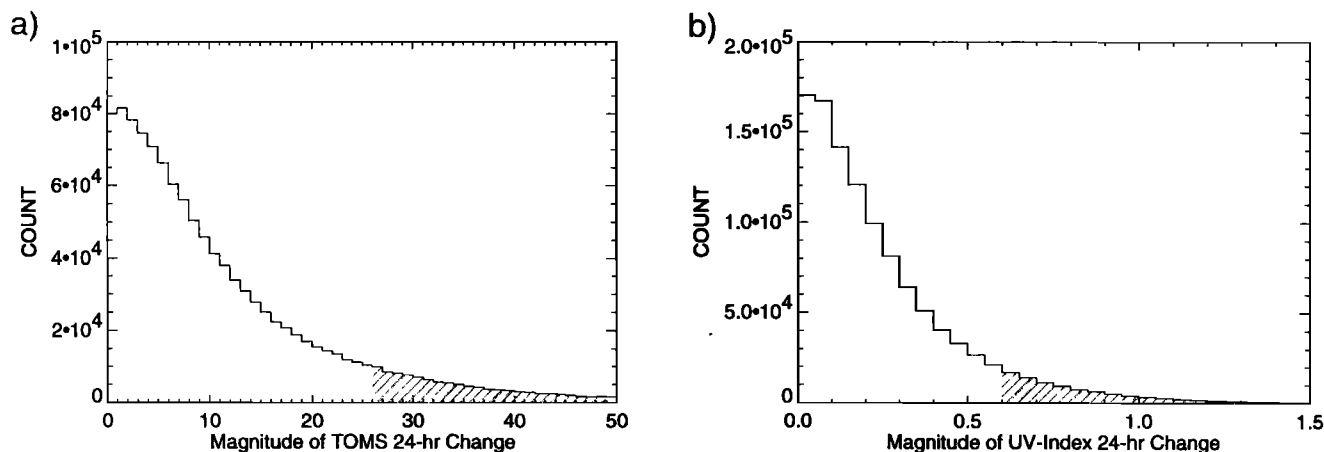


Figure 5. Histograms of accumulated (not hemispherically averaged as in Figure 4) 24-hour changes in summertime (June–July) (a) Ω and (b) resulting UV index for the NH HD-gridded TOMS data from Figure 4. UV index values were derived at each HD grid point by using the parameterized scheme of Austin *et al.* [1994]. Shaded regions indicate upper 10%.

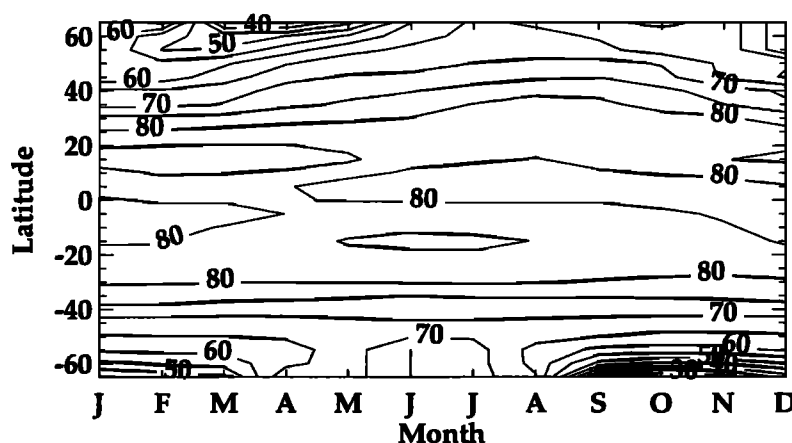


Figure 6. Climatology (1980-1992) of zonally averaged monthly mean cloud versus no-cloud ratios (expressed in percent) of 310-nm daily exposures. These data represent a subset of the UVB data from *Herman et al.* [1996] that incorporated footprint measurements of TOMS Ω and 380-nm reflectivity to derive cloud versus no-cloud UVB.

(not latitudinally weighted) 24-hour changes in summertime (June-July) Ω and resulting clear-sky UV index for the NH HD-gridded TOMS data from Figure 4. The UV index values were derived at each HD grid point by using the parameterized scheme of *Austin et al.* [1994]. Shaded regions indicate the upper 10% of cases; for Ω , 10% of daily variabilities are greater than 26 DU (approximately 7-8% of background Ω). Variabilities greater than 50 DU (15% of background Ω) are rare but not improbable during summer months. In midlatitudes a -15% change in Ω during summer translates to approximately a +20% change in computed clear-sky UV index (see, for example, *Long et al.* [1996]).

Even the largest of such clear-sky daily UV variabilities are generally smaller than UV variabilities caused by unpredictable transient clouds. As an example, Figure 6 shows a 1980-1992 climatology of zonally averaged monthly mean cloud versus no-cloud ratios (in percent) of daily 310-nm UV exposures. These data represent a subset of the UVB data from *Herman et al.* [1996] that incorporated concurrent footprint measurements of TOMS Ω and 380-nm reflectivity to derive cloud and no-cloud ground-level UVB. Figure 6 compares closely with a previous study by *Lubin and Jensen* [1995] (e.g., their Figure 1 line plot for January, April, July, and October 1989), even though their data, length of data set, and technique were uniquely different. Their study incorporated Earth Radiation Budget Experiment (ERBE) radiances, TOVS water vapor, and version 6 TOMS ozone (for 1985).

Figure 6 indicates that in midlatitudes during summer, cloud/no-cloud UVB differences are around 20-30%. These are sizeable changes that will generally be greater than the largest day-to-day percent variabilities in computed clear-sky UVB. Although many current schemes appear to do well in predicting Ω , this study shows that the large UV variabilities caused by transient clouds appear to overwhelm many of the benefits of providing detailed clear-sky UVB forecasts. However, accurate Ω forecasts can currently benefit UVB

predictions in predominantly cloud-free regions such as the U.S. desert southwest and in high-pressure systems that can persist for 1 week or more during stagnant summer weather regimes. As accuracy of cloud predictions improve, Ω forecasts will enhance UVB forecast capabilities.

7. Summary

This study demonstrates that Ω measurements from nadir-viewing SBUV instruments are degraded seriously by horizontal sampling that causes aliasing of detected signals. This is not the case for the new EP and ADEOS high-density side-scanning TOMS spectrometer measurements. As a test a simple Ω prediction model utilizing lower stratospheric temperature as a dynamical surrogate was applied to both Nimbus 7 TOMS and NOAA 11 SBUV2. The results indicated for summer months in both hemispheres ~30-40% error reductions in Ω from persistence for TOMS but, because of aliasing, no significant improvements with SBUV2.

Dynamical parameters (such as lower stratospheric temperatures) are limited in their usefulness to predict next-day Ω because Ω is not a conserved atmospheric tracer. Instead, Ω is a total column measurement and encounters significant day-to-day transport effects, such as column deformity caused by strong wind shears. Ω predictors are most coherent with Ω for medium scales (zonal wavenumbers 4-7) in midlatitudes because of strong year-round baroclinic disturbances associated with the tropospheric wind jets.

Daily variabilities (equivalent to errors in 24-hour persistence forecasting of Ω) in high-resolution (1° latitude \times 1.25° longitude) TOMS midlatitude ozone during summer were shown to sometimes exceed 50 DU, producing daily changes of 20% or greater in computed ground-level clear-sky UV index. However, this study demonstrated that even these large daily changes in measured or predicted clear-sky UV will usually be smaller than daily UV changes associated with transient

clouds. The large UV variabilities induced by transient clouds are presently the dominant factor limiting accurate UVB forecasts. As the accuracy of cloudiness predictions improves in weather forecast models, Ω predictions will enhance UVB forecast capabilities, especially in regions forecast to have reduced cloudiness. Moreover, accurate Ω forecasts can currently benefit UVB predictions in predominantly cloud-free regions such as the desert southwest of the United States and in high-pressure systems that can persist for 1 week or more in stagnant summer weather regimes. Results of the present study show, however, that high-resolution TOMS-like side-scanning Ω observations are required for prediction and monitoring of ozone and UVB, rather than SBUV-type nadir measurements.

TOMS data are made available to anyone via World Wide Web at the TOMS homepage (currently, http://jwocky.gsfc.nasa.gov/#TOMS_Data). Daily data can be obtained directly from this site and cover November 1978 to the present, including near-real time data. The near-real time data come from EP TOMS and are updated approximately every 6 hours.

Acknowledgments. We thank the NASA TOMS Nimbus Experiment and Information Processing Teams for providing the TOMS data. In addition, we wish to thank E. Celarier and D. Larko for their efforts in the development of the UVB products and many helpful discussions. J. L. Stanford was supported in part by National Aeronautics and Space Administration grant NAG5-1519.

References

- Allen, D. R., and R. A. Reck, Daily variations in TOMS total ozone data, *J. Geophys. Res.*, **102**, 13,603–13,608, 1997.
- Atkinson, R. J., S. Grainger, and P. M. Udelhofen, A scheme for the routine analysis and deterministic prediction of the global total ozone distribution, *Proc. South. Hem. Meteorol. Conf.*, in press, 1998.
- Austin, J., B. R. Barwell, S. J. Cox, P. A. Hughes, J. R. Knight, G. Ross, P. Sinclair, and A. R. Webb, The diagnosis and forecast of clear sky ultraviolet levels at the Earth's surface, *Meteorol. Appl.*, **1**, 321–336, 1994.
- Bhartia, P. K., R. D. McPeters, C. L. Mateer, L. E. Flynn, and C. Wellemeyer, Algorithm for the estimation of vertical ozone profiles from the backscattered ultraviolet technique, *J. Geophys. Res.*, **101**, 18,793–18,806, 1996.
- Burrows, W. R., M. Vallee, D. I. Wardle, J. B. Kerr, L. J. Wilson, and D. W. Tarasick, The Canadian operational procedure for forecasting total ozone and UV radiation, *Meteorol. Appl.*, **1**, 247–265, 1994.
- Fleig, A. J., R. D. McPeters, P. K. Bhartia, B. M. Schlesinger, R. P. Cebula, K. F. Klenk, S. L. Taylor, and D. F. Heath, *Nimbus 7 solar backscatter ultraviolet (SBUV) ozone product user's guide*, NASA Ref. Publ., 1234, 1990.
- Herman, J. R., P. K. Bhartia, J. Ziemke, Z. Ahmad, and D. Larko, UV-B increases (1979–1992) from decreases in total ozone, *Geophys. Res. Lett.*, **23**, 2117–2120, 1996.
- Hogg, R. V., and A. T. Craig, *Introduction to Mathematical Statistics*, 4th ed., Macmillan, New York, 1978.
- Long, C. S., A. J. Miller, H.-T. Lee, J. D. Wild, R. C. Przywarty, and D. Hufford, Ultraviolet index forecasts issued by the National Weather Service, *Bull. Am. Meteorol. Soc.*, **77**, 729–748, 1996.
- Lubin, D., and E. H. Jensen, Effects of clouds and stratospheric ozone depletion on ultraviolet radiation trends, *Nature*, **377**, 710–713, 1995.
- Madronich, S., The atmosphere and UV-B radiation at ground level, in *Environmental UV Photobiology*, edited by A. R. Young et al., pp. 1–39, Plenum, New York, 1993.
- Randel, W. J., and J. L. Stanford, Observational study of medium-scale wave dynamics in the southern hemisphere summer, I, Wave structure and energetics, *J. Atmos. Sci.*, **42**, 1172–1188, 1985.
- Spankuch, D., and E. Schulz, Diagnosing and forecasting total column ozone by statistical relations, *J. Geophys. Res.*, **100**, 18,873–18,885, 1995.
- Stanford, J. L., and J. R. Ziemke, A practical method for predicting midlatitude total column ozone from operational temperature fields, *J. Geophys. Res.*, **101**, 28,769–28,773, 1996.
- Ziemke, J. R., and J. L. Stanford, Correlation of total ozone with dynamical variables, *Proc. 18th Quadrenn. Ozone Symp.*, in press, 1998.
- P. K. Bhartia, J. R. Herman, and J. R. Ziemke, Code 916, Chemistry and Dynamics Branch NASA Goddard Space Flight Center, Greenbelt, MD 20771. (e-mail: bhartia@carioca.gsfc.nasa.gov, herman@tparty.gsfc.nasa.gov, ziemke@jwocky.gsfc.nasa.gov)
- J. L. Stanford, Department of Physics and Astronomy, Iowa State University, Ames, IA, 50011. (e-mail: stanford@iastate.edu)

(Received August 12, 1997; revised November 10, 1997; accepted November 11, 1997.)